ELSEVIER

Surface Science 419 (1998) L100–L106

surface science

Surface Science Letters

Self-assembly of multilayer arrays from Ag nanoclusters delivered to Ag(111) by soft landing

S. Jay Chey, L. Huang, J.H. Weaver *

Department of Materials Science and Chemical Engineering, University of Minnesota, Minneapolis, MN 55455, USA

Received 25 August 1998; accepted for publication 22 September 1998

Abstract

Three-dimensional Ag nanostructures containing 150–600 000 atoms were created on Xe multilayers at 50 K. They were delivered to Ag(111), strained Ag(111), and Ag/Si(111)-($\sqrt{3}\times\sqrt{3}$)R30° following Xe desorption, and they were imaged with a scanning tunneling microscope after warming to room temperature. On Ag(111), they wetted the surface and produced hexagonal multilayer epitaxial islands that decayed via step–step contact while maintaining a constant mean terrace width of $\approx$11 Å. On strained Ag(111), there was wetting and an irregular hexagonal footprint but strain stabilized the multilayers by changing the energetics of atom exchange and step fluctuation. On Ag/Si(111)-($\sqrt{3}\times\sqrt{3}$)R30°, contacts were established but decay was not observed.

Keywords: Clusters; Nanostructures; Scanning tunneling microscopy; Silicon; Silver; Surface morphology

There is considerable interest in the synthesis and characterization of nanometer-sized clusters [1,2]. Such materials are known to have novel properties such as quantum confinement [3] and catalytically active surfaces [4]. Clusters can also exhibit adhesion-induced wetting [5], melting point depression [6], and volume-dependent yield strength [7], and their reduced dimension offers opportunities to study sintering [8] and mass transport at nanometer scales [9].

Special procedures must be implemented to produce three-dimensional clusters on reactive supports since they are not the equilibrium thermodynamic structure. We have developed a method that uses a Xe buffer layer as a temporary surface on which clusters can form during physical vapor deposition at 50 K [10,11]. This buffer layer prevents reaction with the substrate during cluster growth and allows the formation of novel overlayer–substrate composites. Previously, we demonstrated that buffer-layer-assisted growth produces Ag nanostructures that can be delivered to Si(111) and that their size and density can be adjusted by varying the Xe layer thickness [12]. Here, we prepare Ag nanostructures for delivery to surfaces where their interactions and their decay can be measured at room temperature with scanning tunneling microscopy (STM) under clean conditions. Those delivered to Ag(111) orient themselves epitaxially to produce multilayer islands that decay with a constant terrace width. Those delivered to strained Ag(111) also wetted the surface but were stabilized by the higher chemical potential of the terraces. On Ag/Si(111)-($\sqrt{3}\times\sqrt{3}$)R30°, contact

* Corresponding author. Fax: +1 612 6256043.

0039-6028/98/$ – see front matter
PII: S0039-6028(98)00755-9

was established but atom exchange among particles was negligible. These results demonstrate that deposition of clusters derived from tens of thousands of atoms produces novel structures whose stability and properties can be tuned by adjusting surface conditions.

The experiments were performed in ultrahigh vacuum (base pressure $<5\times10^{-11}$ Torr) to assure contamination-free contacts. Si(111)-7×7 samples were cleaned and characterized in the STM measurement chamber before being transferred to a cold finger stage in a connected chamber. They were then cooled to 50 K and ten monolayers of Ag were deposited. Annealing to $\approx$700 K for 10 min produced two surface structures in which areas of Ag/Si(111)-($\sqrt{3}\times\sqrt{3}$)R30° coexisted with $\approx$500 Å high Ag(111) islands [13]. A third type of substrate, strained Ag(111), was obtained by depositing 20 Å of Ag on Si(111)-7×7 at 50 K and allowing imperfect planarization to occur at room temperature [13]. These starting samples were then cooled to 50 K and exposed to ultrapure Xe to grow a buffer layer[1]. Subsequent exposure to a flux of Ag atoms from a thermal source produced clusters on the Xe (deposition rate $\approx$0.6 Å min^{-1} at $<1\times10^{-10}$ Torr). Finally, Xe was desorbed and the clusters were delivered at $\approx$68 K when the samples were removed from the cold stage by a room-temperature transfer fork. Imaging was done at room temperature, starting $\approx$1 h after cluster delivery.

Fig. 1a–c shows STM images obtained after cluster delivery to unstrained Ag(111). The amount of Ag deposited onto the Xe was 1 Å for Fig. 1a and c and 0.4 Å for Fig. 1b. Increasing the buffer layer thickness from 24 to 180 to 500 ML increased the mean size of the clusters delivered to the surface because of cluster coalescence during Xe desorption. From results obtained following delivery to Si(111)-7×7, where the nanostructures were stable [12], the as-delivered clusters would have contained 150–8000 atoms for Fig. 1a, 4000–70 000 atoms for Fig. 1b, and 10 000–600 000 atoms for Fig. 1c. Although this delivery process is the ultimate in soft landing, the images of Fig. 1 show substantial atomic rearrangement after contact was established, regardless of cluster size.

In Fig. 1a, the clusters lost memory of their initial structure because the barriers for atom rearrangement were small [15]. Instead, the one- or two-layer high islands approximated the equilibrium hexagonal shape expected for a close-packed homoepitaxial layer. Islands such as I and II were in the process of merging to reduce step lengths and kink energies. The rate of decay of second layer islands was dictated by the barriers for atom evaporation from upper layer steps and transfer to the lower terrace [15]. Repetitive imaging showed island coalescence as a result of island diffusion [16–18]. In the later stages, larger islands grew at the expense of smaller islands.

Fig. 1b and c show the consequence of delivering larger clusters separated by $\approx$1000 Å (densities 1.9×10^{10} and 7×10^{9} cm^{-2}). Imaging revealed multilayer islands derived from close-packed (111) planes. The six-layer island in the center of Fig. 1b is depicted in Fig. 2a and b. The corner-to-corner dimension of the top layer was about 120 Å, and it was derived from $\approx$40 000 atoms. Significantly, the average slope along $\langle\bar{2}11\rangle$ for these multilayer islands was 12.3° (standard deviation $\pm$1.2°), as measured by STM for many islands probed with different tips. This corresponds to a mean terrace width of 11 ± 1 Å or 3.8 ± 0.3 atoms, as drawn in Fig. 2b. With such narrow terraces, it was not possible to resolve individual steps. Although these islands decayed with time, they maintained a constant mean terrace width while doing so. This can be seen from Fig. 2c which summarizes the slopes measured at different times for multilayer islands that included some of those from the sample of Fig. 1c. The values given were found by averaging slopes measured for each island over the six $\langle\bar{2}11\rangle$ directions. This reduced the effects of drift in the imaging and fluctuations in island shape. The largest island analyzed was 27 ML high with a top layer dimension of 140 Å corner to corner for $\approx$600 000 atoms.

Homoepitaxial multilayer islands will decay to

[1] The dose can be converted to layer thickness by correcting the ion gauge reading for its sensitivity to Xe and assuming a sticking coefficient of 1.0 for Xe on Xe at 50 K. A 10 L dose would increase the thickness by 1 ML where 1 ML is the atom density of Xe(111). See Ref. [14].

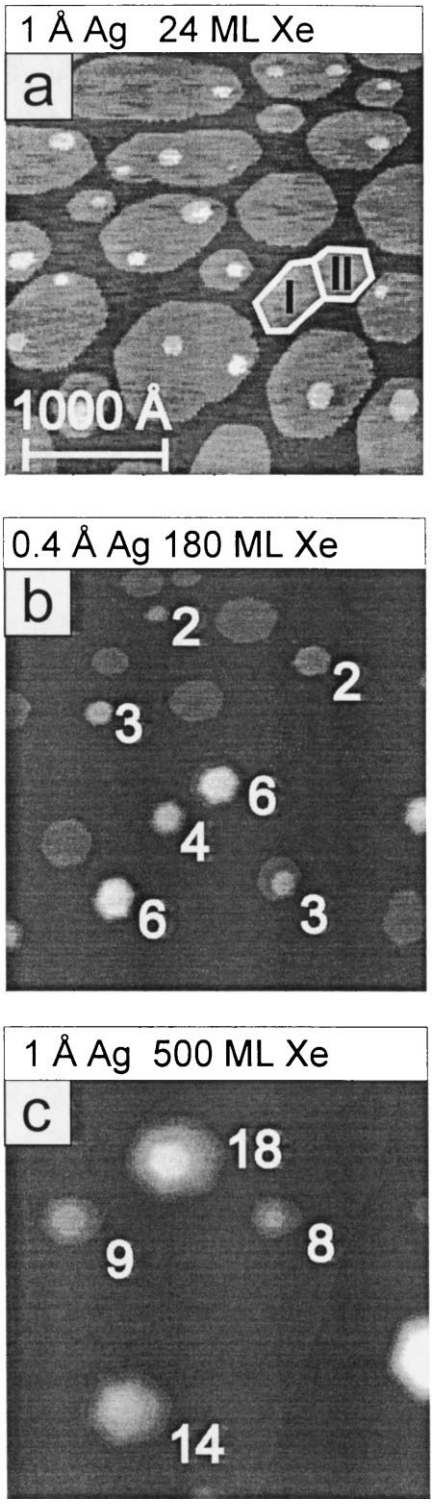

Fig. 1. (a) STM image showing overlayer formation on Ag(111) using Ag clusters grown by buffer layer assembly. The clusters, derived from 150–8000 atoms, lost memory of their original shape, wet the surface, and produced multilayer islands that coalesced and coarsened. (Room temperature imaging with sample bias +1.5 V). (b) As in (a) with growth from clusters containing up to ≈70 000 atoms. (c) As in (a) with clusters as large as 600 000 atoms. The heights of representative multilayer islands are given in (b) and (c). Although these islands were in the process of decaying, they maintained nearly constant ≈11 Å terrace widths. This represents a novel form of self-assembly and quantum confinement.

reduce the free energies associated with the total step length. The images of Fig. 3a–d show such decay for an intermediate-sized island. In this case, the starting configuration was produced by depositing 0.1 Å Ag on 250 ML Xe on Ag(111) and the first useful images were acquired ≈24 h after cluster delivery. Island A in Fig. 3a was 6 ML high and consisted of ≈41 000 atoms. Island B was 3 layers high, consisted of ≈36 000 atoms, and had a much larger footprint and a more irregular shape. Between Fig. 3a and b, island B decayed to a single layer island. Between Fig. 3b and c, island A decreased in height from 6 to 5 ML. Images obtained at intermediate times showed the top layer of A to shrink before eventually disappearing. The decay of island A can be quantified by plotting the number of atoms in its base layer as a function of time, Fig. 3e. The rate of base layer decay during the first 1500 min was relatively gradual, $\approx 0.02\ s^{-1}$ but it increased dramatically as the base decreased and was $\approx 0.28\ s^{-1}$ during the final 250 min. During the last 250 min, it decayed from 3 to 2 layers and disappeared. The base layer decay rate reflects the transfer of atoms from upper layers to the base layer and the exchange of atoms between the base layer and surrounding islands or steps. In turn, the exchange with other islands is controlled by their distribution and relative footprints [19]. The net effect was that, although the total number of atoms initially in island A was greater than in B, island B had a larger footprint and was more stable against atom evaporation. Accordingly, B grew at the expense of A and other smaller islands. The rate of decay of island A increased as its footprint decreased, as is evident in Fig. 3e. Atom exchange also accounted for the

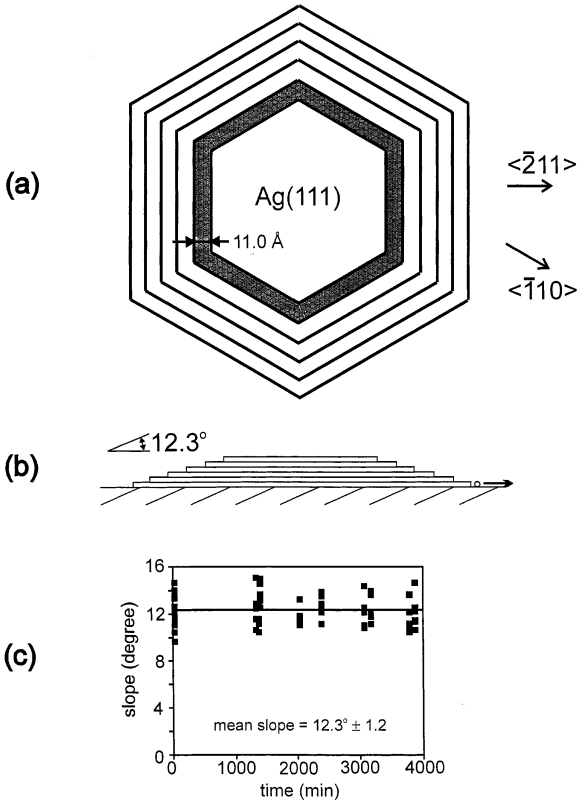

Fig. 2. (a) Top and (b) side view of a multilayer island of Ag that had wet the Ag(111) surface. The average slope was $12.3 \pm 1.2^{\circ}$ and this was maintained during island decay (c). The mean terrace width was 11 ± 1 Å (3.8 ± 0.3 atom diameters).

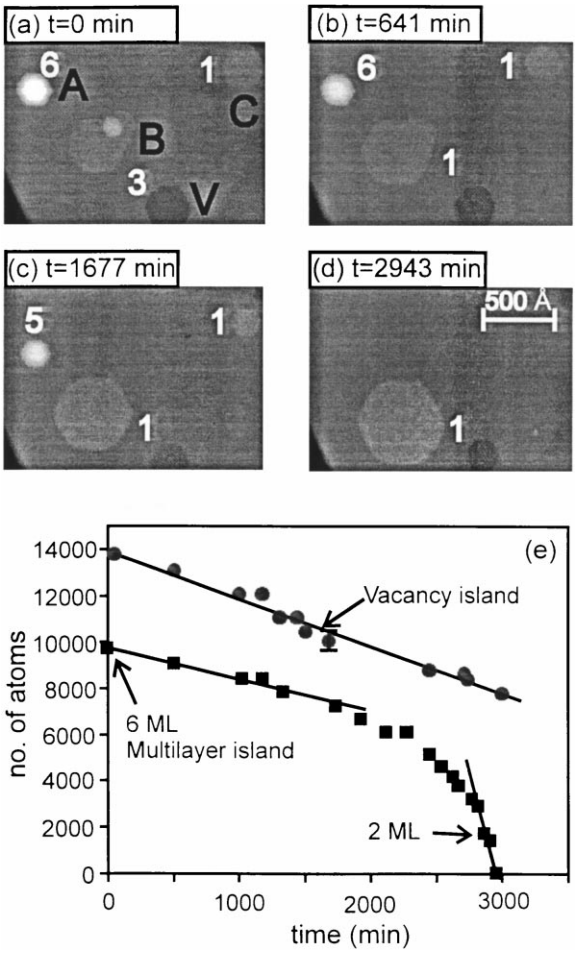

Fig. 3. (a)–(d) Representative images showing the decay of multilayer island A, the growth and shape change of B, and the partial filling of the vacancy island. Sample bias 1.0 V, tunneling current 0.5 nA. (e) The number of atoms in base layer of island A during its decay and the rate of filling of the vacancy island.

disappearance of single-layer island C. From Fig. 3, there was also partial filling of the vacancy island, V. The filling rate, deduced from the straight line in Fig. 3e, was $0.034\ s^{-1}$. This linear decrease is in agreement with observations by Morgenstern et al. [15] and was limited by the Schwoebel–Ehrlich barrier. Note that the edge of the extended (111) crystallite on which these clusters were deposited can be seen at the lower left corner of the images. It too would have played a role in the redistribution of Ag atoms. Moreover, larger-scale scans of the area included by Fig. 3 showed equivalent decay for clusters that were not regularly scanned, and no tip effects were observed (tunneling current 0.5 μA, bias +1 V).

Insight into the mechanism by which these multilayer islands decay can be gained from a recent study of islands on Cu(111) [20]. Giesen et al. proposed that an island would engage in random motion via rapid edge diffusion and that this island would occasionally touch a descending step. For two-layer islands, they observed that the rate of decay of the top island was much slower than that of the base island when the top island was small compared with the base. When the top island established contact with the descending step, however, the rate of top island decay increased by about two orders of magnitude, an effect they related to a reduction in the Schwoebel–Ehrlich

barrier for interlayer mass transport. For a three-layer island, the bottom layer shrank as a result of exchange of atoms with other structures, and this shrinkage increased the likelihood of contact with upper layers. Decay of this three-layer island ultimately produced a pair of Cu(111) terraces with a mean width of 3.72 ± 0.18 atom diameters.

The multilayers that we have produced by cluster deposition represent an extension to much greater height compared with the three-layer islands of Giesen et al. For our multilayers, we observed terraces with mean widths of 3.8 atom diameters at 296 K, which compares favorably with those for Cu(111) at 314 K. Steps on both Ag(111) and Cu(111) will exhibit thermally activated fluctuations, and these fluctuations represent the physical process that allows step contact to occur. The effective decay rate is then a combination of these rates, namely base island decay, upper terrace decay involving a Schwoebel–Ehrlich barrier, and ledge-contact decay. Base island decay is the limiting factor, ledge contact reduces the effect of the Schwoebel–Ehrlich barrier [20], and step fluctuations account for the terrace widths.

It is intriguing to envision the evolution of these large clusters, starting with their initial contact on the ideal Ag(111) terrace. These clusters extend up to 600 000 atoms and, assuming a spherical shape, would have radii up to ≈ 135 Å. Wetting would reflect significant atom rearrangement. The fact that the multilayers appear to be hexagonal and their decay behavior closely parallels that for thin multilayers grown by atom deposition on Cu(111) indicates that they are nearly defect free since defects or dislocations would pin the steps.

To examine how island stability would depend on the perfection of the substrate, we formed and delivered Ag nanostructures to strained Ag(111) layers grown on Si(111)-7×7. The starting surfaces were prepared by depositing 20 Å of Ag at 50 K onto Si(111)-7×7. Warming to room temperature allowed the unstable low-temperature structures to transform into more uniform multilayer films. Imaging such surfaces showed terraces that were ≈ 2000 Å in width with steps that reflected the miscut of the underlying Si substrate. Although Fig. 4a was obtained after cluster delivery to such a surface, the area shown in the inset

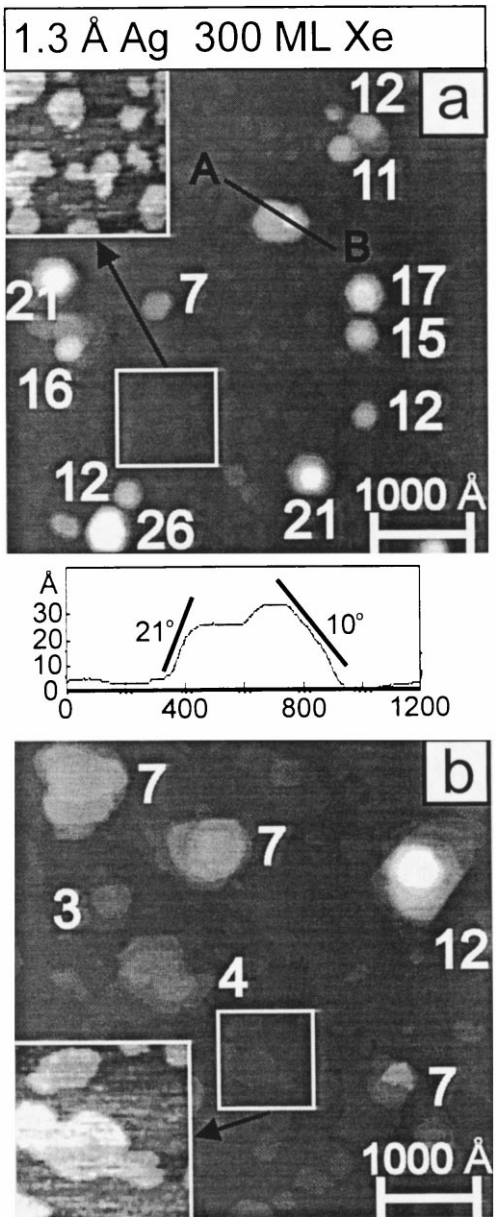

Fig. 4. (a) Image of multilayer Ag islands on strained Ag(111) on Si(111) showing arrested changes in morphology compared with Fig. 1 because of substrate imperfections. The area in the inset shows the surface prior to cluster delivery was rich in monolayer islands and pits whose steps were pinned. The line-scan shows a multilayer island whose cap was probably stabilized by a dislocation. (b) Image obtained after annealing (a) at 180°C for 7 min, showing improved surface quality but still limited island decay.

was representative of the starting surface, as shown in Ref. [13]. The terraces were decorated with monolayer islands and pits that were several hundred ångströms in size. These features were irregular though $\langle \bar{2}11 \rangle$ segments could be identified. The unique structure of this surface reflects the fact that the ≈ 20 Å thick film (8 layers) is strained and is rich in dislocations and other structural imperfections related to low temperature crystallization on Si(111)-7×7 [13]. Monolayer step fluctuations were not observed because these imperfections tend to pin the steps [21]. This substrate is then in a higher energy thermodynamic state than that of Fig. 1.

Fig. 4a was obtained after 1.3 Å of Ag was deposited onto a 300 ML Xe layer condensed on the Ag film and after the clusters that formed were delivered and imaged at room temperature. The bright features were derived from clusters made up of 5000–400 000 atoms. These features wetted the surface and exhibited footprints with $\langle \bar{2}11 \rangle$ steps, as for deposition on unstrained Ag(111), but there was greater deviation from hexagonal shape. Heights ranged up to 26 layers, and slopes ranged from ≈ 10 to $\approx 35^\circ$. Results like this were obtained with different amounts of Ag and different buffer layer thicknesses. Significantly, the morphology remained unchanged after more than 24 h of continuous scanning. Even multilayer islands such as that crossed by the line A–B in Fig. 4a were stable, though the line scan shows the island to be of two heights, with a major part 13 ML thick and 4 ML higher cap.

To test further the stability of these structures, we annealed the sample represented by Fig. 4a at 180°C for 7 min. From the inset of Fig. 4b, the monolayer terrace islands coarsened significantly as the quality of the Ag film itself improved. The multilayer islands associated with the deposited clusters also coarsened (initial density $\approx 9 \times 10^9$ cm^{-2}, final density $\approx 4 \times 10^9$ cm^{-2}). For them, the terrace widths were much larger than in Fig. 1 or Fig. 2 and slopes were typically 1–10°. Annealing at ≈ 240°C resulted in phase separation into the lower energy states of Ag(111) and Ag/Si(111)-$(\sqrt{3} \times \sqrt{3})$R30°.

From the above, it is clear that substrate quality plays a profound role in the stabilization of overlayer structures, even for a homoepitaxial system. For the unstrained multilayer, the limiting process in decay involved evaporation from the base layer island and atom incorporation in a larger island. For the strained surface, our results show that monolayer steps of the surface itself do not exhibit step fluctuations over the time scale of our measurements and atom exchange was insufficient to coarsen the islands or vacancy pits, in contrast to what occurs on unstrained surfaces. Moreover, the strained Ag(111) surface has structural defects such as grain boundaries and dislocations that will change the chemical potential on the terrace and the activation energy for diffusion [22]. Since atom exchange is suppressed on the defective surface, the self-assembly of upper level terraces on the multilayer islands is also limited. The stability of the multilayers, especially such as crossed by line A–B in Fig. 4c, can be related to imperfections within the islands themselves. With an imperfect surface as a template, the deposited cluster will wet but will incorporate imperfections. This will frustrate step diffusion and will account for the more ragged steps and the variation in slopes observed.

Finally, we investigated the morphologies of Ag nanocrystals on the Ag/Si(111)-$(\sqrt{3} \times \sqrt{3})$R30°. In this case, the shape and distribution of the nanocrystals showed no significant difference from those on Si(111)-7×7, and they could be approximated as hemispheres [12]. The contacts formed with the surface were sufficient to prevent tip-induced manipulation of the added Ag structures. No changes in the morphology were observed with time. This is reasonable since the phase separation that produced the Ag/Si(111)-$(\sqrt{3} \times \sqrt{3})$R30° structure implies that the energy of an extra Ag adatom on the surface would be high.

In this paper, we showed that novel structures can be prepared by depositing large clusters and controlling the surface on which they land. We demonstrated a self-assembly process involving periodic terraces and steps for multilayers islands due to wetting and thermal relaxation. It should be possible to stabilize these structures by cooling to lower temperature after formation or by

exposing to an adsorbate that would hinder step fluctuations. It is interesting to speculate whether stabilized terraces could be used as templates for growth or for short-period diffraction gratings. Quantum-confined electronic states on these terraces should exhibit unique dispersion relations. It should be possible to engineer such mound structures for a variety of materials, exploiting what is known about surface free energies, Schwoebel–Ehrlich barriers, and kinetic control of microstructures. Studies that would show the earlier stages of wetting could be done at low temperature where thermally activated processes are retarded.

Acknowledgements

This work was funded by the Office of Naval Research. We thank K. Nakayama and B.Y. Han for stimulating discussions.

References

[1] H. Gleiter, Prog. Mater. Sci. 33 (1989) 223–315.
[2] L.D. Marks, Rep. Prog. Phys. 57 (1994) 603.
[3] M. Zacharias, P. Fauchet, Appl. Phys. Lett. 71 (1997) 380.
[4] R.M. Lambert, G. Pacchioni (Eds.), Chemisorption and Reactivity on Supported Clusters and Thin Films: Towards an Understanding of Microscopic Processes in Catalysis, NATO ASI Series E, vol. 331, Kluwer, Dordrecht, 1997.
[5] U. Landman, W.D. Luedtke, N.A. Burnham, R.J. Colton, Science 248 (1990) 454.
[6] S.L. Lai, J.Y. Guo, V. Petrova, G. Ramanath, L.H. Allen, Phys. Rev. Lett. 77 (1996) 99.
[7] J.D. Kiely, J.E. Houston, Phys. Rev. B 57 (1998) 12588.
[8] M. Yeadon, J.C. Yang, R.S. Averback, J.W. Bullard, D.L. Olynick, J.M. Gibson, Appl. Phys. Lett. 71 (1997) 1631.
[9] S.J. Chey, J.E. Van Nostrand, D.G. Cahill, Phys. Rev. Lett. 76 (1996) 3995.
[10] G.D. Waddill, I.M. Vitomirov, C.M. Aldao, J.H. Weaver, Phys. Rev. Lett. 62 (1989) 1568.
[11] J.H. Weaver, G.D. Waddill, Science 251 (1991) 1444.
[12] L. Huang, S.J. Chey, J.H. Weaver, Phys. Rev. Lett. 80 (1998) 4095.
[13] L. Huang, S.J. Chey, J.H. Weaver, Surf. Sci. Lett. 416 (1998) L1101.
[14] J.W. Bartha, U. Barjenbruch, M. Henzler, J. Phys. C 19 (1986) 2459.
[15] K. Morgenstern, G. Rosenfeld, E. Laesgaard, F. Besenbacher, G. Comsa, Phys. Rev. Lett. 80 (1998) 56.
[16] J.-M. Wen, J.W. Evans, M.C. Bartelt, J.W. Burnett, P.A. Thiel, Phys. Rev. Lett. 73 (1994) 2591.
[17] K. Morgenstern, G. Rosenfeld, B. Poelsema, G. Comsa, Phys. Rev. Lett. 74 (1995) 2058.
[18] W.W. Pai, A.K. Swan, Z. Zhang, J.F. Wendelken, Phys. Rev. Lett. 79 (1997) 3210.
[19] G. Schulze Icking-Konert, M. Giesen, H. Ibach, Surf. Sci. 398 (1998) 37.
[20] M. Giesen, G. Schulze Icking-Konert, H. Ibach, Phys. Rev. Lett. 80 (1998) 552.
[21] J.F. Wolf, B. Vincenzi, H. Ibach, Surf. Sci. 249 (1991) 233.
[22] H. Brune, H. Roder, C. Boragno, K. Kern, Phys. Rev. Lett. 73 (1994) 1955.